

Ab initio Yb₂ ground state potential revisited

Giorgio Visentin,^{1, a)} Alexei A. Buchachenko,^{1, 2, b)} and Paweł Tecmer^{3, c)}

¹⁾*Skolkovo Institute of Science and Technology, Skolkovo Innovation Center, Moscow 121205, Russia*

²⁾*Institute of Problems of Chemical Physics RAS, Chernogolovka, Moscow Region 142432, Russia*

³⁾*Institute of Physics, Faculty of Physics, Astronomy and Informatics, Nicolaus Copernicus University in Toruń, Grudziadzka 5, 87-100 Torun, Poland*

The ground-state interaction potential of ytterbium dimer is investigated at eXact 2-component core-correlated CCSD(T) level of *ab initio* theory in the complete basis set limit with extensive augmentation by diffuse functions. For the basis set of double- ζ quality, the comparison is made with the four-component relativistic finite-nuclei CCSD(T) calculations to identify the contraction of the dimer bond length as the main unrecoverable deficiency of the scalar-relativistic approximation. Empirical constraint on the number of bound vibrational energy levels of the ¹⁷⁴Yb₂ dimer is accounted for by employing the model semianalytical potential function [M. Borkowski et al. Phys. Rev. A **96**, 063405 (2017)] containing the scale and shift parameters. Using the best *ab initio* data as its short-range part, we estimated the equilibrium parameters of Yb₂ dimer as $R_e \in [4.45, 4.55]$ Å and $D_e = 745 \pm 10$ cm⁻¹. Furthermore, we demonstrated that the model potential provides an accurate and flexible reference for future research in constraining short-range gravity-like forces by ultracold atomic spectroscopy.

^{a)}Electronic mail: giorgio.visentin@skoltech.ru

^{b)}Electronic mail: a.buchachenko@skoltech.ru

^{c)}Electronic mail: ptecmer@fizyka.umk.pl

I. INTRODUCTION

Recent advances in ultracold atomic physics have brought weakly-bound ytterbium dimer, never detected spectroscopically at room temperature, up to forefront fundamental and applied research. Atomic energy level scheme convenient for laser confinement, cooling, and narrow band excitation was explored in the ultraprecise Yb frequency standard for time measurements¹ and relativistic geodesy applications². Yet, further refinement has been predicted for a clock based on Yb dimer³. Numerous photoassociation spectroscopy (PAS) studies in the degenerate Yb gases made significant insight in ultracold collision dynamics, long-range interactions, and exotic diatomic states⁴⁻¹⁴. A variety of naturally abundant isotopes of bosonic and fermionic nature and relatively large mass made Yb dimer very attractive for studying the mass-dependent non-Born-Oppenheimer effects and the short-range gravity-like interactions^{11,15}. Specifically, it has been shown¹⁶ that unprecedented 500 Hz accuracy of the PAS data on the near-threshold rovibrational levels of Yb₂ is enough to improve the constraints on the non-Newtonian gravity forces by two orders of magnitude, providing that the accuracy of the underlying theoretical model is refined. The effects beyond the Born-Oppenheimer (BO) approximation related to non-adiabatic interactions with excited states should provide a major share of such refinement. An important step towards realistic and reliable *ab initio* description of the lowest excited states of Yb dimer has been made recently¹⁷. However, even the ground-state $^1\Sigma_g^+$ BO potential is not known with due certainty, being well-defined only in the long-range region, where the dispersion coefficients from accurate *ab initio* calculations¹⁸⁻²¹ have been further refined by fitting to PAS data and scattering length measurements^{6,11,22}. The lack of experimental data directly focusing on the attractive well of Yb dimer requires more accurate and reliable *ab initio* reference data.

For decades, the scalar-relativistic (SR) coupled cluster singles, doubles, and non-iterative triples method, CCSD(T), in combination with small-core relativistic pseudo-potentials stood as a reliable approach for *ab initio* modeling of weakly interacting potential energy surfaces composed of heavy elements. The ground-state Yb₂ potential obtained within this framework²³ required only 3% adjustment of the BO binding energy D_e (from 724 to 743 cm⁻¹) to provide the best fit to the benchmark PAS data¹¹. On the other hand, the sensitivity of this data to the behavior of the potential in the well region is rather weak.

Indeed, lower in quality but still satisfactory fits were obtained earlier with model potentials completely different from the *ab initio* predictions^{6,22}. That is why the results of the recent all-electron scalar-relativistic CCSD(T) calculations¹⁷ sound alarming. Prediction of 20% smaller D_e calls in question the uniqueness of the models developed to fit PAS data and assess non-Newtonian gravity forces in Refs. 11,16.

Consistent *ab initio* treatment of all the effects physically important for the interaction of Yb atoms is not feasible. Predominantly dispersion bonding character implies extensive recovery of the dynamic electron correlation, core-valence and outer-core one included, in a highly saturated basis sets augmented with the diffuse component. The SR CCSD(T) method with extrapolation to the complete basis set (CBS) limit provides the only tractable means to meet these requirements. It disregards, however, essential contributions from high-order cluster excitations. Furthermore, vectorial relativistic effects, first of all, spin-orbit (SO) coupling, are not negligible for lanthanides²⁴. To estimate them quantitatively, one should contrast the SR results with the sophisticated four-component calculations, far more restrictive with regards to basis size and extent of correlation treatment. The importance of some factors mentioned above had already been estimated for Yb dimer by Mosyagin et al.²⁵ by using the CCSD(T), 4-electron full configuration interaction and relativistically-corrected density functional theory (DFT) methods.

The *ab initio* study reported in the present paper pursues the refinement of the ground-state Yb₂ BO potential in three ways. First, we performed a series of all-electron scalar-relativistic CCSD(T) calculations with the so-called eXact 2-component (X2C) Hamiltonian²⁷⁻³², extensive treatment of the core correlation and the CBS extrapolations with different diffuse augmentations. These results resolve the controversy in the previous all-electron and effective core potential calculations and supply the reference short-range part to the global model potential. Second, for the first time we carried out the four-component relativistic CCSD(T) calculations with the outer-core correlation treatment and the basis set of double- ζ quality. One-to-one comparison with the X2C CCSD(T) results reveals remarkable Yb–Yb bond length’s contraction, the effect not fully captured by the scalar-relativistic calculations. Finally, we combined the newest converged X2C CCSD(T) short-range potentials with accurately known long-range dispersion tail of the model potential function suggested in Ref. 11. Accounting for empirical constraint on the number of bound vibrational levels of the ¹⁷⁴Yb₂ dimer and uncertainty of the relativistic contraction, we provided conservative

bounds to the equilibrium parameters of Yb dimer. As a result, we proposed a new accurate and flexible potential function for further refinement of the beyond-Born-Oppenheimer models.

II. *AB INITIO APPROACHES*

A. Spin-orbit coupling and scalar-relativistic calculations with DIRAC

All the CCSD(T) calculations were carried out using the DIRAC19 relativistic software package³³ utilized a linear $D_{\infty h}^*$ symmetry, the valence double- ζ basis set of Dyall³⁴, and the Gaussian nuclear model, if not stated otherwise. The calculations kept $4f$, $5p$, and $6s$ spinors (orbitals) correlated (leaving 48 inner electrons within the core per atom, c48 option, for brevity), and all virtuals were active.

We assessed the performance of various relativistic Hamiltonians. Specifically, these include (i) the four-component Dirac–Coulomb Hamiltonian, in which the $(SS|SS)$ integrals were approximated by a point charge model³⁵ denoted as 4C-DC, (ii) the spin-free Dirac–Coulomb Hamiltonian denoted as SF-DC²⁶, and (iii) the spin-free X2C Hamiltonian^{27–32} denoted as SF-X2C. An additional set of calculations was performed for the SF-X2C Hamiltonian with the point-charge nuclear model. That allowed us for direct comparison with the SR calculations carried out in the MOLPRO software package³⁶ described below.

As we aimed to analyze the relativistic effects on the equilibrium parameters, the grid of 27 internuclear distances R were restricted to 5–20 a_0 (roughly 2.6–10.6 Å) interval. Counterpoise (CP) correction³⁷ was applied imposing the $C_{\infty v}^*$ point group symmetry.

B. Scalar-relativistic calculations with MOLPRO

The sequence of the Dunning-type correlation-consistent polarized valence cc-pVnZ basis sets with the cardinal numbers $n = D, T, Q$ (hereinafter for brevity VnZ) contracted for use with the X2C scalar-relativistic Hamiltonian³⁸ was used. To compensate for the lack of optimized diffuse augmentation, we added one or two primitives for each symmetry type with the exponents continuing the sequence of basis exponents in an even-tempered manner with the default parameters of the MOLPRO 2015.1 program package³⁶. In what follows, these options are denoted as e1 or e2, respectively. The 3s3p2d2f1g set of bond function

(bf)³⁹ placed at the midpoint of Yb–Yb distance was also used for the same purpose. The restricted Hartree–Fock reference functions were obtained in the D_{2h} symmetry group for the dimer and the C_{2v} group for the Yb atom in the full dimer basis set with the X2C Hamiltonian. Two series of the CCSD(T) calculations correlated $5s$, $5p$, $4f$, and $6s$ orbitals (c46 option, 46 electrons within the core per atom) and, in addition, $4s$, $4p$, and $4d$ orbitals (c28 option). Refs. 17,21 indicate that the correlation of deeper shells has a negligible effect on the potential well parameters and dispersion coefficients of the dimer. The energy convergence threshold was set to $10^{-10} E_h$ in all calculations.

Counterpoised CCSD(T) potentials were computed on a non-uniform grid of 57 internuclear distances spanning the range from 2 to 50 Å. At distances longer than 25 Å, erratic non-smooth variations of energies were detected. This prevents a firm determination of the dominant C_6 dispersion coefficient by fitting and limits the accuracy of interaction energies by 0.05 cm^{-1} . Parameters of all interaction potentials were determined using the cubic spline interpolation.

Establishing the connection to DIRAC results, a few auxiliary X2C CCSD(T) calculations were made on the shorter grid introduced above. They used the c48 option for core correlation and original VDZ, uncontracted VDZ (uVDZ) and uncontracted Dyall double- ζ bases without further augmentation.

C. Complete basis set extrapolation

The X2C CCSD(T) energies computed with the VDZ, VTZ, and VQZ basis sets were extrapolated to the CBS limit using two three-point formulas. The first (CBS1 hereinafter) is the mixed exponential-Gaussian one^{40,41}

$$E(n) = E_{\text{CBS}} + Be^{-(n-1)} + Ce^{-(n-1)^2}, \quad (1)$$

while the second (CBS2) is the two-term inverse power function by Martin and Taylor^{42,43}

$$E(n) = E_{\text{CBS}} + B/(n + 1/2)^4 + C/(n + 1/2)^6, \quad (2)$$

where $E(n)$ are the energies computed with the basis set of the certain cardinal number n and E_{CBS} is the extrapolated energy value. Both formulas contain linear extrapolation parameters B , C and are compatible with the CP correction⁴⁴.

III. RESULTS

A. Assessment of the scalar-relativistic approximation

Table I compares the parameters of the CCSD(T) c48 Yb₂ interaction potentials, namely, inflection point at zero kinetic energy σ and equilibrium parameters R_e , D_e , as obtained for the basis sets of double- ζ quality without further augmentations. Implementations of the X2C Hamiltonian in DIRAC and MOLPRO packages gave identical results for the Dyall basis set. The MOLPRO calculations with the Dunning-type basis showed significantly weaker bonding. For the predominantly dispersion interaction we are dealing with here, this indicates the poorer quality of the VDZ basis even in its uncontracted form. The contraction alters D_e marginally, but reduces R_e by almost 0.02 Å. Such a significant increment should persist for the VnZ sets of higher cardinal numbers and thus cannot be recovered by extrapolation to the CBS limit. The calculations with DIRAC package demonstrated that a slight increase of the binding energy due to SO coupling and finite-nuclei effects is nearly canceled by the SF X2C Hamiltonian. By contrast, related contraction of R_e by 0.01 Å reflects the main deficiency of the scalar-relativistic approximation (see the Supplementary material for tabulated *ab initio* potential energies with different relativistic Hamiltonians).

TABLE I. Parameters of the CCSD(T) c48 potentials calculated with the double- ζ basis sets. Calculations with DIRAC used Gaussian nuclear model unless stated otherwise.

Method	Package	σ (Å)	R_e (Å)	D_e (cm ⁻¹)
X2C VDZ	MOLPRO	4.080	4.741	475.4
X2C uVDZ	MOLPRO	4.062	4.727	478.0
X2C Dyall	MOLPRO	4.022	4.694	531.9
SF-X2C Dyall point charge	DIRAC	4.022	4.694	531.9
SF-X2C Dyall	DIRAC	4.018	4.692	533.0
SF-DC Dyall	DIRAC	4.024	4.694	526.0
4C-DC Dyall	DIRAC	4.012	4.686	532.3

B. Basis set convergence of scalar-relativistic results

The SF X2C CCSD(T) calculations are efficient enough to achieve the convergence of the Yb_2 potential with respect to the basis set saturation and the core correlation treatment. Both factors can be assessed using the CBS extrapolations of the Dunning-type VnZ results with different diffuse augmentations. Figure 1 shows the convergence of the equilibrium distance R_e and well depth D_e to the CBS limit for the VnZ , $VnZe1$, and $VnZbf$ series. Two former exhibit slow but monotonous convergence and weak dependence on the core choice. By contrast, calculations with bond functions converge much faster but not in a regular manner and exhibit a somewhat stronger dependence on the core choice. The inset in the Figure indicates that the difference between the results of two extrapolation formulas, Eqs. (1) and (2), does not exceed 1%. In what follows, only extrapolated X2C potentials will be discussed. The full set of related *ab initio* data can be found in the supplemental materials to this paper.

Table II lists the values of interaction potential parameters extracted in the CBS limit. It also gives the semiclassical estimates of the number of bound vibrational energy levels ν obtained with the potential model introduced in Sec. III C (*vide infra*). The variations of all parameters are in line with the trends depicted in the Figure 1. Diffuse augmentations are necessary to better recover dispersion interactions. Addition of the second atomic-centered diffuse primitive set is excessive, while the use of bond functions provides somewhat larger binding energy and shorter equilibrium distance. The correlation of the $4s4p4d$ shells affects the interaction potential marginally, almost within the uncertainty of the CBS extrapolations by Eqs. (1) and (2). Overall, the data collected in the Table II estimate the converged X2C CCSD(T) equilibrium parameters as $R_e = 4.59 \pm 0.01 \text{ \AA}$ and $D_e = 650 \pm 10 \text{ cm}^{-1}$.

The results of the previous SR X2C CCSD(T) calculations are presented in Table II as well. The only available all-electron calculations from Ref. 17 underestimate the present D_e values by ca. 10% and overestimate R_e by 0.07 \AA . Besides the minor difference in the applied scalar-relativistic Hamiltonians (X2C vs. Douglas–Kroll–Hess of the second order), this mismatch should be attributed to the lack of the diffuse functions in the correlation-consistent atomic natural orbital (ANO) basis set used therein. The best ANO result falls between the present VTZe1 and VQZ results despite the ANO basis was used in its uncontracted form.

The potential from Refs. 11,23 is based on the small-core effective core potential ECP28MWB⁴⁵

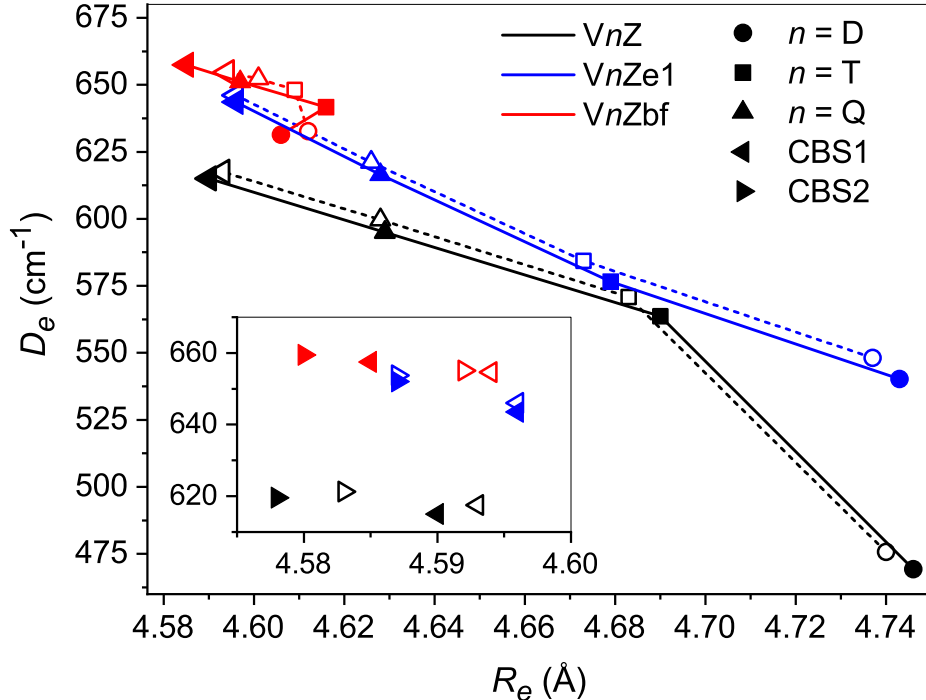


FIG. 1. Convergence of the equilibrium distance R_e and binding energy D_e to the CBS limit using the CBS1 extrapolation formula (1). Colors distinguish augmentations of the basis sets, symbol shapes – basis cardinal numbers. Solid symbols with solid lines and open symbols with dashed lines represent the c28 and c46 results, respectively. Inset enlarges the CBS limit region and shows the results of the CBS2 extrapolation (2) as well.

combined with the corresponding ANO basis⁴⁶ augmented by the specially designed atom-centered diffuse function set⁴⁷ and the bf set³⁹ simultaneously. It implies stronger bonding of Yb atoms than the present series does, namely, the binding energy is larger by 11% and the equilibrium distance is shorter by 1.5%. This difference should be attributed to the uncertainty of effective core potential description of the inner shells, as is corroborated by the calculations by Wang and Dolg with the same basis but different diffuse augmentation⁴⁸.

Mosyagin and co-workers²⁵ investigated the bonding of Yb atoms using the 28-electron generalized relativistic effective core potential (GRECP) and a series of supplementary basis sets. Only four outer electrons were correlated in their reference CCSD(T) calculations with the largest basis. Correction to outer core correlation (OC, equivalent to the present c46 core option) was evaluated with a smaller basis. Contributions of the iterative triple and quadruple cluster excitations (iTQ) and the SO coupling were estimated by invoking the

TABLE II. Parameters of the SR CCSD(T) *ab initio* Yb₂ interaction potentials from the present CBS1 calculations and literature, in Å and cm⁻¹ units unless otherwise specified. Present CBS2 results are given in parentheses.

Method	σ	R_e	D_e	ν (a.u.)
VnZ c46	3.916 (3.911)	4.593 (4.583)	617.5 (621.2)	66.99 (67.10)
VnZe1 c46	3.907 (3.900)	4.596 (4.587)	646.1 (653.8)	68.15 (68.45)
VnZe2 c46	3.907 (3.901)	4.598 (4.590)	646.9 (654.1)	68.20 (68.48)
VnZbf c46	3.906 (3.905)	4.594 (4.592)	654.6 (655.0)	68.35 (68.37)
VnZ c28	3.915 (3.908)	4.590 (4.578)	615.0 (608.4)	66.90 (67.05)
VnZe1 c28	3.906 (3.898)	4.596 (4.587)	643.6 (652.0)	68.12 (68.48)
VnZbf c28	3.896 (3.893)	4.585 (4.580)	657.5 (659.5)	68.54 (68.63)
ANO c28 ¹⁷		4.665	580	
ECP28MWB ^{11,23}	3.870	4.522	723.8	70.97
ECP28MWB ⁴⁸		4.549	742	
28e GRECP+OC ²⁵		4.683	642	
28e GRECP +OC+iTQ ²⁵		4.615	767	
28e GRECP +OC+iTQ+SO ²⁵		4.582	787	

full configuration interaction and relativistically corrected DFT, see original paper for more details²⁵. The CCSD(T)+OC and CCSD(T)+OC+iTQ results are quoted in the Table II. The D_e value from the former calculations is reasonably close to the present VnZe1 c46 CBS limit, but R_e is greatly overestimated. The effects of the higher-order cluster correction on equilibrium distance and binding energy amount to 1.5% and 20%, respectively. The SO correction (CCSD(T)+OC+iTQ+SO) adds extra 0.7% and 2.5%.

While the converged SR X2C CCSD(T) values of $R_e \approx 4.60$ Å and $D_e \approx 650$ cm⁻¹ bound the true potential parameters from above and below, respectively, the opposite bounds can only be guessed combining the data from different sources. If we apply the percentage changes due to higher-order cluster excitations and SO coupling found by Mosyagin et al.²⁵, R_e shrinks down to 4.5 Å and D_e increases to 810 cm⁻¹. Alternative estimations can be obtained by making the artificial CBS extrapolations of the double- ζ 4C-DC CCSD(T) relativistic results using the extrapolation coefficients B and C in Eqs.(1), (2) from the

corresponding SR X2C CCSD(T) c48 series. This leads to $R_e \approx 4.53 \text{ \AA}$ and $D_e \approx 680 \text{ cm}^{-1}$, or $\approx 4.52 \text{ \AA}$ and $\approx 710 \text{ cm}^{-1}$ if the effect of diffuse function augmentation is accounted for. The iTQ correction from Ref. 25 finally gives $R_e \approx 4.45 \text{ \AA}$ and $D_e \approx 835 \text{ cm}^{-1}$.

The same artificial extrapolation applied to the double- ζ SF-DC CCSD(T) results in estimates of the combined effect of SO coupling and finite nuclear size at equilibrium as 9 cm^{-1} , twice as small as reported by Mosyagin and co-workers.²⁵

C. Model potential and semiclassical scaling

As indicated above, neither the only experimental datum – mass-spectrometric estimation of the dissociation energy⁴⁹ as $1400 \pm 1400 \text{ cm}^{-1}$, nor the estimations of harmonic frequency, empirical⁵⁰ 21 cm^{-1} and upper bound for excited state in inert matrices⁵¹ of 48 cm^{-1} , help us to assess the *ab initio* results. Very helpful, however, is the fact that ultracold PAS and scattering length data can be fitted reasonably well only with the potential supporting 72 bound vibrational levels for the $^{174}\text{Yb}_2$ dimer at zero rotational momentum^{6,11}.

To explore this constraint, we represented the global Yb_2 interaction potential $V(R)$ in the model semianalytical form¹¹

$$V(R) = [1 - f(R)]sV_{\text{SR}}(R) + f(R)V_{\text{LR}}(R), \quad (3)$$

where the short-range part V_{SR} designates the *ab initio* points interpolated by cubic splines and the long-range part contains two lowest dispersion interaction terms

$$V_{\text{LR}}(R) = -C_6/R^6 - C_8/R^8, \quad (4)$$

as the PAS data is not sensitive to the next C_{10} term¹¹. The switching function has the fixed form

$$f(R) = \begin{cases} 0, & \text{if } R \leq a \\ \frac{1}{2} + \frac{1}{4} \sin \frac{\pi x}{2} (3 - \sin^2 \frac{\pi x}{2}), & \text{if } a < R < b \\ 1 & \text{if } R > b, \end{cases} \quad (5)$$

with $x = [(R-a)+(R-b)]/(b-a)$, $a = 10 a_0$ (5.292 \AA), $b = 19 a_0$ (10.054 \AA). The dispersion coefficients were taken as $C_6 = 1937.27$ and $C_8 = 226517 \text{ a.u.}$ ¹¹, respectively. The scaling parameter s is adjustable. If set to unity, Eq.(3) describes the interpolation of the original *ab initio* points at $R \leq a$.

Instead of using elaborate fitting to PAS energies and scattering lengths performed in Ref. 11 to scale the ECP28MWB CCSD(T) potential²³, we resorted here to much simpler semiclassical procedure described in Ref. 52. The semiclassical phase at zero kinetic energy is given by

$$\Phi = \frac{1}{\hbar} \int_{\sigma}^{\infty} \sqrt{2\mu[-V(R)]} dR, \quad (6)$$

where μ is the reduced mass of the Yb dimer. Here, following the analysis of Borkowski et al.¹¹, we used the atomic reduced mass of the $^{174}\text{Yb}_2$ dimer. Note that Eqs.(3), (5) permit analytical integration of the phase from $R = b$ to infinity that greatly facilitates accurate numerical evaluation of the integral (6). The effective number of the bound vibrational levels is given by $[\nu]$, $\nu = \Phi/\pi + 3/8$. The ν values for the original ($s = 1$) SR X2C CCSD(T) CBS potentials are given in Table II. The best of them consistently support 68 bound levels.

TABLE III. Scaling factors s and scaled binding energies (cm^{-1}) of the CBS1 potentials for the $^{174}\text{Yb}_2$ dimer. Results for the CBS2 potentials are given in parentheses.

Potential	s	sD_e
VnZ c46	1.233 (1.226)	761.2 (761.8)
VnZe1 c46	1.172 (1.157)	757.2 (756.7)
VnZe2 c46	1.169 (1.156)	756.5 (755.8)
VnZbf c46	1.162 (1.161)	760.7 (760.1)
VnZ c28	1.237 (1.229)	761.0 (761.8)
VnZe1 c28	1.173 (1.157)	755.2 (754.3)
VnZbf c28	1.153 (1.148)	757.9 (757.0)
ECP28MWB ¹¹	1.027	743.0 \pm 2.4

Next, we vary parameter s until ν becomes greater than 72. The resulting values of s and scaled binding energies are listed in Table III. It is evident that the constraint on the bound level projects the original potentials, whose binding energies vary by 45 cm^{-1} , to a much narrower interval of 8 cm^{-1} , with a mean value of 758 cm^{-1} . The minimum scaling coefficient required for the VnZbf c28 potential indicates 15% increase of the binding energy, of which about 2% can be attributed to the relativistic effects and the rest, about 90 cm^{-1} , to the higher-order cluster contributions (QED and other non-Born-Oppenheimer effects omitted). Both corrections are smaller than those derived by Mosyagin et al.²⁵.

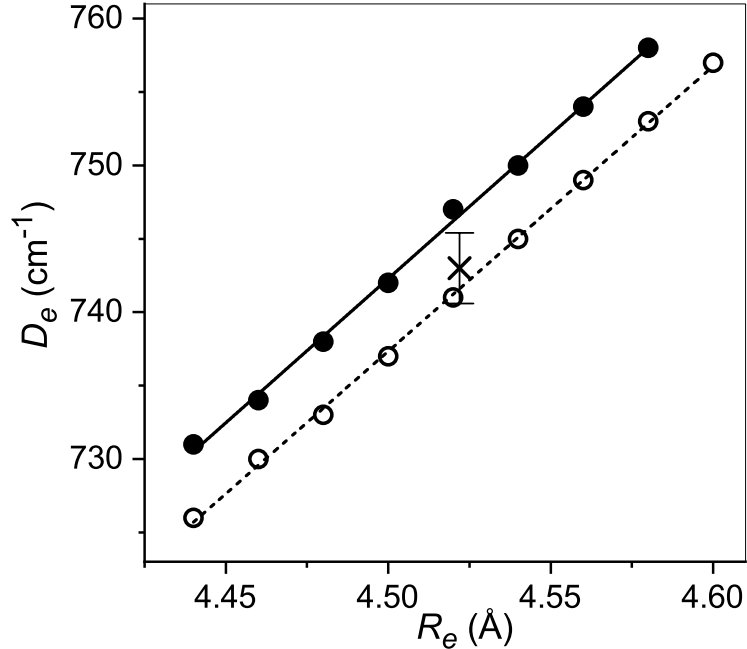


FIG. 2. Correlation of the scaled binding energy and shifted equilibrium distance of the Yb_2 interaction potential. Solid and open symbols correspond to the $VnZbf$ c28 and $VnZe2$ c46 reference X2C CCSD(T) CBS1 *ab initio* data, respectively, whereas lines represent the linear fits. Cross indicates the scaled Born-Oppenheimer result from Ref. 11.

Previous analysis revealed that the SR X2C CCSD(T) CBS calculations significantly overestimate the dimer equilibrium distance. The shift of the potential towards a shorter range should obviously affect the scaling by increasing the phase. We introduced the shift parameter $d \in [0, 0.16]$ Å and replaced the *ab initio* part of the model function (3) by the shifted potential $V_{\text{SR}}(R - d)$. For each d , the scaling parameter s was found using the same criterion as above. Figure 2 shows the results in terms of shifted and scaled equilibrium parameters for the representative cases of the CBS1 $VnZe2$ c46 and $VnZbf$ c28 *ab initio* potentials. Position and depth of the potential well are correlated linearly with the coefficient $-195 \pm 4 \text{ cm}^{-1}/\text{Å}$. It is also evident that the scaling of the present potentials agrees well with the results of Ref. 11, where the ECP28MWB potential²³ was used as the reference.

Close correspondence of the scaled parameters and strong correlation between them indicate that all the *ab initio* potentials have very similar shape in the minimum region. We believe that the Figure 2 identifies the most probable ranges for equilibrium parameter

variation, i.e., $R_e \in [4.45, 4.55] \text{ \AA}$ and $D_e = 745 \pm 10 \text{ cm}^{-1}$.

IV. CONCLUDING REMARKS

First, present calculations set the scalar-relativistic CCSD(T) benchmark for the ground-state potential of Yb dimer. Achieving the convergence with respect to basis set saturation and extent of correlation treatment, we estimated its X2C CCSD(T) equilibrium parameters as $R_e = 4.59 \pm 0.01 \text{ \AA}$ and $D_e = 650 \pm 10 \text{ cm}^{-1}$. These values lie in between two previous CCSD(T) evaluations, one with the all-electron SR description¹⁷, another with the small-core effective core potential²³. The former suffers from the lack of the diffuse functions in the ANO basis set employed; the latter reveals the deficiency of the ECP28MWB potential, which, artificially but fortuitously, significantly exaggerates Yb–Yb bonding. Second, the first four-component relativistic CCSD(T) calculations performed in a double- ζ basis generally support the validity of the X2C approximation. Our study show that overestimation of the Yb–Yb bond length is a major error which arises from a systematic deficiency of the *cc-pVnZ* sets as well as from relativistic contraction.

Finally, we used the global semianalytical potential function suggested in Ref. 11 to merge the *ab initio* points with accurately known long-range dispersion tail. It permitted the semiclassical scaling of the calculated potentials to obey the empirical constraint on the number of bound vibrational levels supported by the $^{174}\text{Yb}_2$ potential. The scaling of all the variety of X2C CCSD(T) CBS results gives the binding energies within the very narrow interval, $D_e = 758 \pm 4 \text{ cm}^{-1}$. We estimated that vectorial SO and finite nuclei effects amount to about 10% of the energy gain from scaling. The rest should be attributed to omitted higher-order cluster excitations. To take into account the error in the bond length inherent to the X2C CCSD(T) reference, we introduced the potential shift parameter and arrived to the final estimates $R_e \in [4.45, 4.55] \text{ \AA}$ and $D_e = 745 \pm 10 \text{ cm}^{-1}$. They justify the previous best fit to photoassociation spectroscopy data¹¹ obtained with the ECP28MWB reference that yielded $R_e = 4.52 \text{ \AA}$ and $D_e = 743.0 \pm 2.4 \text{ cm}^{-1}$. As the *ab initio* calculations fix the shape of the short-range potential, shift and scale parameters are well correlated. Thus, the present study provides an accurate and flexible functional description of the ground-state Yb_2 dimer for future use in the beyond-Born-Oppenheimer models of the photoassociation spectra for searching mass-dependent effects related to non-Newtonian gravity.

SUPPLEMENTAL MATERIAL

See the supplemental material for tabulated CCSD(T) results with different relativistic Hamiltonians and X2C CCSD(T) calculations described in Secs. III A, and II B and III B, respectively.

ACKNOWLEDGMENTS

We thank Mateusz Borkowski, Piotr Żuchowski, and Dariusz Kędziera for many helpful discussions. Financial support by the Russian Science Foundation under project no. 17-13-01466 is gratefully acknowledged. P.T. thanks an OPUS 17 research grant of the National Science Centre, Poland, (no. 2019/33/B/ST4/02114) and a scholarship for outstanding young scientists from the Ministry of Science and Higher Education.

REFERENCES

- ¹A. D. Ludlow, M. M. Boyd, J. Ye, E. Peik, and P. O. Schmidt, *Rev. Mod. Phys.* **87**, 638 (2015).
- ²W. F. McGrew, X. Zhang, R. J. Fasano, S. A. Schaeffer, K. Beloy, D. Nicolodi, R. C. Brown, N. Hinkley, G. Milani, M. Schioppo, T. H. Yoon, and A. D. Ludlow, *Nature* **564**, 87 (2018).
- ³M. Borkowski, *Phys. Rev. Lett.* **120**, 083202 (2018).
- ⁴S. Tojo, M. Kitagawa, K. Enomoto, Y. Kato, Y. Takasu, M. Kumakura, and Y. Takahashi, *Phys. Rev. Lett.* **96**, 153201 (2006).
- ⁵K. Enomoto, M. Kitagawa, S. Tojo, and Y. Takahashi, *Phys. Rev. Lett.* **100**, 123001 (2008).
- ⁶M. Borkowski, R. Ciuryło, P. S. Julienne, S. Tojo, K. Enomoto, and Y. Takahashi, *Phys. Rev. A* **80**, 012715 (2009).
- ⁷Y. Takasu, Y. Saito, Y. Takahashi, M. Borkowski, R. Ciuryło, and P. S. Julienne, *Phys. Rev. Lett.* **108**, 173002 (2012).
- ⁸S. Kato, S. Sugawa, K. Shibata, R. Yamamoto, and Y. Takahashi, *Phys. Rev. Lett.* **110**, 173201 (2013).

- ⁹D. G. Green, C. L. Vaillant, M. D. Frye, M. Morita, and J. M. Hutson, *Phys. Rev. A* **93**, 022703 (2016).
- ¹⁰Y. Takasu, Y. Fukushima, Y. Nakamura, and Y. Takahashi, *Phys. Rev. A* **96**, 023602 (2017).
- ¹¹M. Borkowski, A. A. Buchachenko, R. Ciuryło, P. S. Julienne, H. Yamada, Y. Kikuchi, K. Takahashi, Y. Takasu, and Y. Takahashi, *Phys. Rev. A* **96**, 063405 (2017).
- ¹²L. Franchi, L. F. Livi, G. Cappellini, G. Binella, M. Inguscio, J. Catani, and L. Fallani, *New J. Phys.* **19**, 103037 (2017).
- ¹³R. Bouganne, M. B. Aguilera, A. Dareau, E. Soave, J. Beugnon, and F. Gerbier, *New J. Phys.* **19**, 113006 (2017).
- ¹⁴G. Cappellini, L. F. Livi, L. Franchi, D. Tusi, D. Benedicto Orenes, M. Inguscio, J. Catani, and L. Fallani, *Phys. Rev. X* **9**, 011028 (2019).
- ¹⁵J. J. Lutz and J. M. Hutson, *J. Mol. Spectrosc.* **330**, 43 (2016).
- ¹⁶M. Borkowski, A. A. Buchachenko, R. Ciuryło, P. S. Julienne, H. Yamada, Y. Kikuchi, Y. Takasu, and Y. Takahashi, *Sci. Rep.* **9**, 14807 (2019).
- ¹⁷P. Tecmer, K. Boguslawski, M. Borkowski, P. S. Żuchowski, and D. Kędziera, *Int. J. Quant. Chem.* **119**, e25983 (2019).
- ¹⁸P. Zhang and A. Dalgarno, *Mol. Phys.* **106**, 1525 (2008).
- ¹⁹M. S. Safronova, S. G. Porsev, and C. W. Clark, *Phys. Rev. Lett.* **109**, 230802 (2012).
- ²⁰S. G. Porsev, M. S. Safronova, A. Derevianko, and C. W. Clark, *Phys. Rev. A* **89**, 012711 (2014).
- ²¹G. Visentin and A. A. Buchachenko, *J. Chem. Phys.* **151**, 214302 (2019).
- ²²M. Kitagawa, K. Enomoto, K. Kasa, Y. Takahashi, R. Ciuryło, P. Naidon, and P. S. Julienne, *Phys. Rev. A* **77**, 012719 (2008).
- ²³A. A. Buchachenko, G. Chałasiński, and M. M. Szczęśniak, *Eur. Phys. J. D* **45**, 147 (2007).
- ²⁴P. Pyykko, *Chem. Rev.* **88**, 563 (1988).
- ²⁵N. S. Mosyagin, A. N. Petrov, and A. V. Titov, *Int. J. Quant. Chem.* **111**, 3793 (2010).
- ²⁶K.G. Dyall, *J. Chem. Phys.* **100**, 2118–2127 (1994).
- ²⁷D. Kędziera, in *Recent Progress in Computational Sciences and Engineering, Lecture Series on Computer and Computational Sciences*, vol. 7A–B (VSP BV-C/O BRILL ACAD PUBL, Leiden, The Netherlands, 2006), *Lecture Series on Computer and Computational Sciences*, vol. 7A–B, pp.252–255.

- ²⁸D. Kędziera and M. Barysz, Chem. Phys. Lett. **446**, 176 (2007).
- ²⁹M. Iliáš and T. Saue, J. Chem. Phys. **126**, 064102 (2007).
- ³⁰J. Sikkema, L. Visscher, T. Saue, and M. Ilias, J. Chem. Phys. **131**, 124116 (2009).
- ³¹W. Liu and D. Peng, J. Chem. Phys. **131**, 031104 (2009).
- ³²D. Peng and M. Reiher, Theor. Chem. Acc. **131**, 1081 (2012).
- ³³T. Saue, R. Bast, A. S. P. Gomes, H. J. A. Jensen, L. Visscher, *et al.*, J. Chem. Phys. **152**, 204104 (2020).
- ³⁴A. S. P. Gomes, K. G. Dyall, and L. Visscher, Theor. Chem. Acc. **127**, 369 (2010).
- ³⁵L. Visscher, Theor. Chem. Acc. **98**, 68 (1997).
- ³⁶H.-J. Werner, P. J. Knowles, G. Knizia, F. R. Manby, and M. Schutz, Molpro: a general-purpose quantum chemistry program package, WIREs Comput. Mol. Sci. **2**, 242 (2012).
- ³⁷S. Boys and F. Bernardi, Mol. Phys. **19**, 553 (1970).
- ³⁸Q. Lu and K.A. Peterson, J. Chem. Phys. **145**, 054111 (2016).
- ³⁹S. M. Cybulski and R. R. Toczyłowski, J. Chem. Phys. **111**, 10520 (1999).
- ⁴⁰K. A. Peterson, D. E. Woon, and T. H. Dunning, Jr., J. Chem. Phys. **100**, 7410 (1994).
- ⁴¹D. Feller and J. A. Sordo, J. Chem. Phys. **112**, 5604 (2000).
- ⁴²J. M. L. Martin, Chem. Phys. Lett. **259**, 679 (1996).
- ⁴³J. M. L. Martin and P. R. Taylor, J. Chem. Phys. **106**, 8620 (1997).
- ⁴⁴M. P. de Lara-Castells, R. V. Krems, A. A. Buchachenko, G. Delgado-Barrio, and P. Villarreal, J. Chem. Phys. **115**, 10438 (2001).
- ⁴⁵M. Dolg, H. Stroll, and H. Preuss, J. Chem. Phys. **90**, 1730 (1989).
- ⁴⁶X. Cao and M. Dolg, J. Chem. Phys. **115**, 7348 (2001).
- ⁴⁷A. A. Buchachenko, G. Chałasiński, and M. M. Szcześniak, Struct. Chem. **18**, 769 (2007).
- ⁴⁸X. Cao and M. Dolg, Mol. Phys. **101**, 1967 (2003).
- ⁴⁹M. Guido and G. Balducci, J. Chem. Phys. **57**, 5611 (1972).
- ⁵⁰P. Goodfriend, Spectrochim. Acta A **40**, 283 (1984).
- ⁵¹S. Suzer and L. Andrews, J. Chem. Phys. **89**, 5514 (1988).
- ⁵²G. F. Gribakin and V. V. Flambaum, Phys. Rev. A **48**, 546 (1993).